Prss16 Is Not Required for T-Cell Development

Saijai Cheunsuk,[1] Zhe-Xiong Lian,[2] Guo-Xiang Yang,[2] M. Eric Gershwin,[2]
Jeffrey R. Gruen,[3] and Christopher L. Bowlus[1]*

*Divisions of Gastroenterology[1] and Rheumatology and Allergy,[2] Department of Internal Medicine,
University of California, Davis, California, and Department of Pediatrics, Yale Child Health
Research Center, Yale University School of Medicine, New Haven, Connecticut[3]*

PRSS16 is a serine protease expressed exclusively in cortical thymic epithelial cells (cTEC) of the thymus, suggesting that it plays a role in the processing of peptide antigens during the positive selection of T cells. Moreover, the human *PRSS16* gene is encoded in a region near the class I major histocompatibility complex (MHC) that has been linked to type 1 diabetes mellitus susceptibility. The mouse orthologue *Prss16* is conserved in genetic structure, sequence, and pattern of expression. To study the role of Prss16 in thymic development, we generated a deletion mutant of *Prss16* and characterized T-lymphocyte populations and MHC class II expression on cortical thymic epithelial cells. *Prss16*-deficient mice develop normally, are fertile, and show normal thymic morphology, cellularity, and anatomy. The total numbers and frequencies of thymocytes and splenic T-cell populations did not differ from those of wild-type controls. Surface expression of MHC class II on cTEC was also similar in homozygous mutant and wild-type animals, and invariant chain degradation was not impaired by deletion of *Prss16*. These findings suggest that *Prss16* is not required for quantitatively normal T-cell development.

Peptide fragments, which are processed from self-proteins within the thymus and presented to developing thymocytes, shape the selection of T-cell receptors (TCR). Positive selection, mediated by cortical thymic epithelial cells (cTEC), selects TCR clones that are capable of engaging peptides bound to self-major histocompatibility complex (MHC) (1, 11, 16). Evidence that a diverse array of self-peptides is required for normal positive selection of the CD4+-TCR repertoire comes from mice in which a single peptide is bound to nearly all MHC class II molecules. In the H2-M-deficient mouse, the class II-associated invariant chain peptide fragment (CLIP) fails to be removed; in the A^{b}EpIi$^-$ transgenic mouse, MHC class II molecules are covalently linked to the MHC class II peptide Eα_{52-68} (5, 13, 31). Although both of these strains select a surprisingly large number of T cells, the T-cell repertoire is altered. Further evidence of the role of self-peptide diversity in positive selection comes from mice expressing transgenic TCR β chains. Nearly all T cells in these mice express the transgenic β chain, but the α chain locus undergoes normal rearrangement and selection (4, 6, 28). Sequence analysis of the parenteral α chains has demonstrated a bias that is severely restricted when selected against a limited diversity of self-peptides (4, 12).

The cellular machinery generating self-peptides in cTEC is unique and likely plays an important role in the selection of the TCR repertoire (25). Unlike professional antigen-presenting cells (APC) and medullary thymic epithelial cells, cTEC efficiently process endogenous antigens but poorly process exogenous antigens (22, 24). In addition, the MHC class II compartment in which peptides are generated and loaded occurs in early stages of endosome formation in cTEC as opposed to late stages of endosome formation in APC (18). Furthermore, the proteolytic enzymes that are required for the degradation of antigenic peptides are unique to cTEC (7, 23). In professional antigen-presenting cells, several proteases have been identified and their roles have been characterized (29, 32). However, cTEC express at least two proteases that are not found in other APC. Cathepsin L, a cysteine protease, is required for complete processing of Ii in cTEC, and mice lacking cathepsin L have impaired development of CD4+ and natural killer T cells (17, 23). PRSS16, also known as thymic specific serine protease, is specifically expressed by cTEC and although its precise role is unknown, its cDNA predicts a protein with similarity to the lysosomal serine peptidase, polycarboxypeptidase, suggesting that it may also play a role in antigen presentation during positive selection (7). Moreover, the *PRSS16* gene is encoded within the telomeric MHC class I region on the short arm of chromosome 6p21 approximately 440 kb from *D6S2223*, a marker that has been linked to type I diabetes and celiac disease susceptibility (21).

To determine the function of *Prss16*, we have generated a strain of mice with a targeted deletion in the *Prss16* gene. In this, our initial study of these mice, we investigated the role of *Prss16* in thymus development, the positive selection of T cells, and the expression of MHC class II by cTEC.

MATERIALS AND METHODS

Mice. Chimeras and *Prss16$^{-/-}$* knockout mouse colonies were bred and maintained under specific-pathogen-free conditions. All mice were used at between 4 and 8 weeks of age. C57BL/6J mice were purchased from the Jackson Laboratory (Bar Harbor, Maine).

Construction of the targeting vector. A 15-kb genomic DNA fragment containing the entire *Prss16* coding sequence was isolated from a 129/Sv mouse lambda phage library and mapped by restriction enzyme digestion and sequencing (9). A 0.9-kb XbaI-HindIII fragment including exons 3 and 4 was subcloned into the NheI and HindIII sites of pTK-Neo. A 6.5-kb fragment including a portion of exon 10, the entire exons 11 and 12, and the 3′ flanking region was generated by PCR amplification with 5S1:F1 (5′-GTGACTATCGATTGTGGC
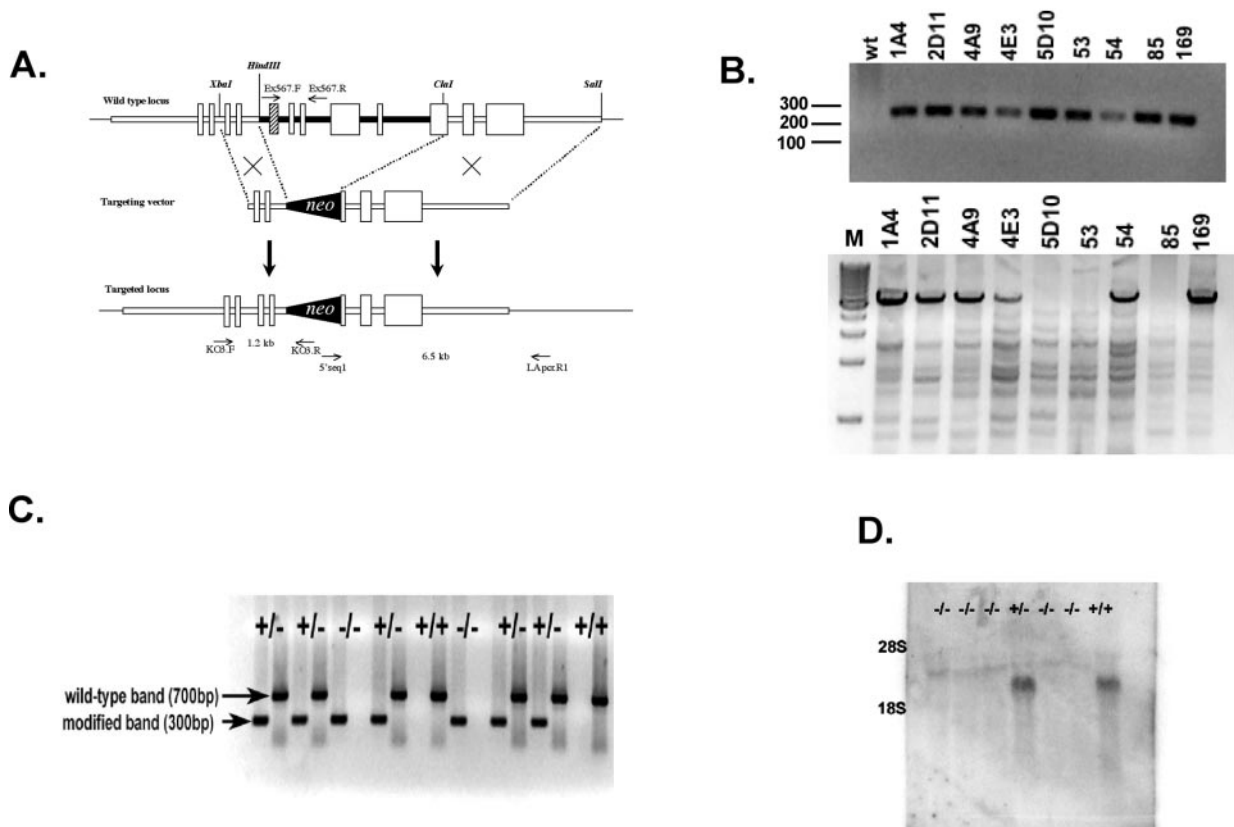
FIG. 1. Targeted disruption of the *Prss16* by homologous recombination. (A) A neomycin resistance cassette was inserted between the HindIII and ClaI sites replacing exon 5 (hatched box), which includes the putative active serine residue, through exon 9 and the 5′ end of exon 10. (B) 5′ (upper panel) and 3′ (lower panel) PCR analysis of ES cells. Primers KO3.F and KO3.R were used to screen for 5′ integration of the targeting vector. 3′ integration was confirmed by PCR with primers 5′seq1 and LApcr.R1. M, molecular weight markers (in hundreds); wt, wild type. (C) Genotype analysis of offspring from heterozygous parents of modified *Prss16*. Tail DNA was used for PCR analyses of the mutant and wild-type alleles with primer pairs KO3.F-KO3.R (lanes 1, 3, 5, 7, 9, 11, 13, 15, 17) and Ex567.F-Ex567.R (lanes 2, 4, 6, 8, 10, 12, 14, 16, 18), respectively. (D) *Prss16*^{−/−} mice do not produce Prss16 mRNA. Northern blot of total thymus RNA from *Prss16*^{−/−}, *Prss16*^{+/−}, and *Prss16*^{+/+} mice probed with a *Prss16* cDNA.

CCAGACAAACTCCT-3′) and 16G4-4R (5′-GTGACTGTCGACCGGCACC ACTACCATCCTCTT-3′). PCR amplification was performed by using *Pfu* Turbo DNA polymerase (Stratagene, La Jolla, Calif.) under the conditions of 1 cycle of 95°C for 3 min; 35 cycles of 95°C for 45 s, 60°C for 45 s, and 72°C for 8 min; and 1 cycle of 72°C for 10 min. The PCR product was separated on a 0.8% agarose gel, purified (QIAquick; QIAGEN, Valencia, Calif.), and subcloned into pPCRScript (Stratagene) modified by eliminating the ClaI site. The 6.5-kb-long arm was digested with SalI and ClaI and cloned into the ClaI and SalI sites of pTK-Neo (Fig. 1A). Homologous recombination with the targeting vector is predicted to delete a total of 6 kb of the *Prss16* gene from exon 5 to exon 10, including the putative active serine site in exon 5.

Generation of ES cell chimeras. The targeting vector was linearized with NotI, and 30 μg of DNA was electroporated into RI embryonic stem (ES) cells. After electroporation, 2×10^6 cells were plated in 100-mm-diameter tissue culture dishes containing a monolayer of G418 resistance embryonic fibroblast feeder cells and selected in 160 μg of G418/μl. Drug-resistant colonies were individually picked, and clones were screened for homologous integration of the 5′ arm by PCR with primers KO3:F1 (5′-GTTCCTGAATCAAGCTGCTCA-3′), KO3:R1 (5′GATCAGCAGCCTCTGTTCCA-3′), and SCKO:F (5′-GCTCTTCATTGCC CTCTCTG-3′). The PCR was performed with 1 cycle at 95°C for 3 min; 35 cycles of 95°C for 60 s, 56°C for 60 s, and 72°C for 90 s; and 1 cycle of 72°C for 6 min. Homologous integration of the 3′ arm was confirmed with primers 5′seq1 (5′-T ACCCGGTAGAATTCTCTAGC-3′) and LApcr:R1 (5′-TTTCAAGTCCTCCC CCTTCAC-3′) to amplify 6.5-kb fragments. By using *Pfu* Turbo DNA polymerase (Stratagene), DNA was amplified under the condition of 1 cycle of 95°C for 3 min; 35 cycles of 95°C for 45 s, 56°C for 45 s, and 72°C for 9 min; and 1 cycle of 72°C for 10 min. Amplification products were separated on a 0.8% agarose gel. Nine homologous recombinants were detected out of the 736 clones screened.

After karyotyping, four homologous recombinant ES cell clones (1A4, 2D11, 54, and 169) were used to generate chimeric mice by microinjection into day 3.5 C57BL/6 blastocysts, which were subsequently transferred into pseudopregnant CD-1 females. The four cell lines generated chimeric mice ranging between 50 and 80% in chimerism, based on the agouti coat color. Male chimeras from each line were mated with C57BL/6 female mice, and offspring with agouti coat color were tested for germ line transmission by PCR of tail DNA. Heterozygotes were intercrossed to produce *Prss16*^{+/+}, *Prss16*^{+/−}, and *Prss16*^{−/−} littermates. The wild-type allele was detected by PCR under the same conditions as the targeted allele with primers Ex567.F (5′-GTTACCGGAAGGAACCTTGG-3′) and Ex567.R (5′-CGCCTTCCTCCACACTCTAC-3′).

Total RNA isolation, probe labeling, and Northern blot analysis. Total RNA was prepared from mouse thymuses by using TriZol reagent (Life Technologies, Rockville, Md.) according to the manufacturer's instructions. Total RNA (20 μg) was separated on a 0.8% formaldehyde agarose gel and transferred onto Hybond-N+ nylon transfer membrane (Amersham Pharmacia Biotech, Piscataway, N.J.). A mouse cDNA IMAGE clone 573004 (GenBank accession no. AI587874) was radiolabeled and hybridized as previously described (7). After two washes (each) in 2× SSC (1× SSC is 0.15 M NaCl plus 0.015 M sodium citrate)–0.1% sodium dodecyl sulfate (SDS) for 20 min at room temperature and 0.2× SSC–0.1% SDS for 20 min at 65°C, the membrane was exposed to a phosphor screen for 48 h at room temperature and analyzed (Molecular Dynamics, Sunnyvale, Calif.).

Pathological evaluation. Necropsies were performed on 6-to-8-week-old mice. Thymuses were removed and fixed in 10% phosphate-buffered formalin and embedded in paraffin. Sections were stained with hematoxylin and eosin stain.

Thymocyte and stromal cell preparation for Western blotting. Thymuses were digested in Hanks' balanced salt solution (HBSS) in the presence of 60 U of collagenase IV (Sigma, St. Louis, Mo.)/ml and 25 Kunitz U of DNase I (Sigma)/

ml. Thymocytes were isolated by disruption of the thymus with a 26-gauge syringe containing HBSS. Thymic stromal cells were collected from the remaining tissues, which were cut into small pieces and left to sediment in HBSS with collagenase for 30 min at 37°C. The suspension was filtered twice through a 100-μm-pore-size mesh and incubated in 5 mM EDTA at 37°C for 30 min. The suspension was then centrifuged on a newborn calf serum cushion (containing 5 mM EDTA) at $50 \times g$ for 3 min. The upper layer was removed, and the cells that had entered the newborn calf serum were harvested by centrifugation at $450 \times g$ for 3 min. Both lymphocytes and thymic stromal cells were washed two times with phosphate-buffered saline (PBS) and collected by centrifugation at $1,500 \times g$ for 5 min at 4°C. Isolated cells were lysed in cell lysis buffer ($1 \times$ PBS, 1% NP-40, 0.5% sodium deoxycholate, and 0.1% SDS) supplemented with complete protease inhibitor mixture (Roche Diagnostics Corp., Indianapolis, Ind.) at 4°C for 30 min. Debris was removed by centrifugation at $15,000 \times g$ for 20 min at 4°C. An equal volume of electrophoresis sample buffer was added to the protein lysate and boiled for 90 s before separation by SDS–12% polyacrylamide gel electrophoresis. Proteins were transferred onto a nitrocellulose membrane, probed with anti-invariant chain (In-1) antibody (kindly provided by A. Rudensky, University of Washington, Seattle) and detected with rabbit anti-rat horseradish peroxidase-conjugated antibody (Santa Cruz Biotechnology, Santa Cruz, Calif.) diluted 1:1,000 and visualized by chemiluminescence (KPL, Gaithersburg, Md.).

Isolation of thymocytes, splenocytes, and low-density thymic epithelial cells for flow cytometry. Thymocytes and splenocytes were isolated from organs dissected and mechanically dissociated in cold 0.2% bovine serum albumin in PBS (BSA-PBS), filtered through 100-μm-pore-size mesh to remove clumps, and washed three times with 10 ml of cold BSA-PBS. The pellet was resuspended in staining buffer (0.2% BSA and 0.01% NaN$_3$ in PBS). Low-density thymic epithelial cells were isolated by discontinuous density gradient centrifugation by a modification of the procedure described by Farr et al. (10). Briefly, thymuses were incubated in 5 ml of HBSS with 60 U of collagenase IV (Sigma)/ml and 25 Kunitz U of DNase I (Sigma)/ml and minced with scissors. Digestion was carried out at 37°C for 15 min, and then the sample was flushed through a 21-gauge needle. The cell suspension was filtered through a 100-μm-pore-size mesh to remove clumps and washed two times with 0.2% BSA-PBS. The resulting cell suspension from two to four thymuses was pooled in 6 ml of Percoll with a density of 1.01, layered onto a 1.05 cushion, and centrifuged for 20 min at $750 \times g$. Cells at the interface were harvested, washed twice with 0.9% NaCl, and resuspended in fluorescence-activated cell sorter (FACS) staining buffer.

Immunofluorescent staining and flow cytometry. Phycoerythrin-conjugated anti-CD4 and FITC-conjugated anti-CD8 antibodies were purchased from Santa Cruz Biotechnology. FITC-conjugated M5/114.15.2 (MHC class II) antibody was purchased from Miltenyi Biotec (Auburn, Calif.). Allophycocyanin-biotinylated conjugated anti-BP1, phycoerythrin-conjugated HL3 (CD11c) and anti-CD25, allophycocyanin-conjugated anti-CD4, Cy5.5-conjugated anti-CD8, and FITC-conjugated anti-CD44 and anti-TCR β were purchased from PharMingen (San Diego, Calif.). Cells were analyzed by using a FACSCalibur flow cytometer (Becton Dickenson). Typically, 100,000 events were recorded for splenocyte and thymocyte analysis, and 50,000 events were recorded for the thymic stromal cell analysis.

T-lymphocyte activation assay. Splenocytes were prepared under sterile conditions, resuspended in 5 ml of red blood cell lysis buffer (eBioscience, San Diego, Calif.) and incubated for 5 min at room temperature, followed by the addition of 30 ml of sterile PBS. Cells were washed with PBS and resuspended in RPMI 1640 supplemented with 10% fetal bovine serum, 2 mM L-glutamine, and 50 μM β-mercaptoethanol. Cells (2.5×10^6/well) were plated in 96-well plates precoated with 10 μg of anti-mouse CD3/ml and incubated in 5% CO$_2$ at 37°C for 48 h. PBS and 2.5 μg of concanavalin A (Sigma)/ml were used for negative and positive controls, respectively. Cells were rinsed with PBS, and fresh medium was added with 20 μl of MTT [3-(4,5-dimethylthiozol-2-yl)-2,5-diphenyl tetrazolium bromide] buffer (Sigma) followed by incubation at 37°C for 4 h. Cells were lysed overnight with 50 μl of 20% SDS–50% dimethyl formamide. The difference in the absorbance at 570 nm between stimulated and unstimulated cells was calculated.

RESULTS

Generation of homologous mutant mice with a mutation in the *Prss16* gene. To define the role of *Prss16*, we generated a null allele of the *Prss16* gene by homologous recombination in ES cells. The targeting vector was designed to insert a *neo* selection cassette into the *Prss16* gene and delete exons 5, 6, 7, 8, 9, and part of exon 10 (Fig. 1A). The *neo* insertion interrupts

the *Prss16* coding sequence at amino acid 112 and deletes the putative catalytic serine residue in exon 5.

After electrophoresis of the linearized targeting vector, RI ES cells were selected with G418. Out of 736 neomycin-resistant ES cell clones analyzed, 9 clones carried a disruption of the 5′ end and 6 clones had disruption of both the 5′ and 3′ ends (Fig. 1B). Four of the correctly targeted ES clones were injected into CD1 blastocysts, and all clones generated chimeras that transmitted the disrupted *Prss16* allele through the germ line. The *Prss16*$^{+/-}$ mice of both sexes were normal and fertile compared to their wild-type littermates. Animals derived from all ES cell clones displayed similar phenotypes. The results presented were generated from the mouse line derived from the 1A4 ES cell clone.

***Prss16*-deficient mice are viable and fertile.** Breeding among *Prss16*$^{+/-}$ mice produced offspring with Mendelian ratios of *Prss16*$^{+/+}$, *Prss16*$^{+/-}$, and *Prss16*$^{-/-}$ genotypes that did not differ significantly from those expected ($P = 0.5$) (Fig. 1C). Of 271 viable offspring, 53 (19.6%) were wild type, 145 (53.5%) were heterozygous, and 73 (26.9%) were homozygous, indicating that *Prss16* does not cause embryonic lethality.

To confirm that the targeted allele does not produce any significant *Prss16* transcript, RT-PCR (data not shown) and Northern blot analysis were performed on total thymus RNA from 4-week-old animals (Fig. 1D). No *Prss16* message could be detected by either method in comparison with the *Prss16*$^{+/-}$ and *Prss16*$^{+/+}$ animals, thus confirming the absence of the *Prss16* transcript in *Prss16*$^{-/-}$ animals.

Prss16$^{-/-}$ mice appeared phenotypically normal and were indistinguishable from their heterozygous and wild-type littermates. In addition, an analysis of tissues of wild-type, heterozygous, and homozygous littermates revealed no consistent abnormalities in gross or histopathological findings. In particular, the morphology of the thymus was normal and showed no difference in size or weight among genotypes (data not shown). Mating of *Prss16*$^{-/-}$ mice produced litters of normal size and progeny that appeared phenotypically normal, indicating that homozygous mutant mice are fertile as well.

***Prss16* functioning in invariant chain and MHC class II expression.** We determined whether *Prss16* is required for Ii degradation or MHC class II expression by comparing *Prss16*$^{-/-}$ mice to their wild-type and heterozygous littermates. Ii is degraded in a stepwise process to peptide fragments of 41, 31, and 10 kDa. By using anti-Ii antibody (In-1), thymic stromal cells showed no difference in Ii degradation products between the two groups of animals, suggesting that *Prss16* is not required for this process (Fig. 2A).

We also studied the surface expression of MHC class II on cTEC identified as BP-1$^+$CD4$^-$CD11c$^-$ cells within the population of low-density thymic cells. Surface staining of MHC class II of *Prss16*$^{-/-}$ mice, as measured by relative fluorescence intensity, was similar to that of wild-type and heterozygous mice (Fig. 2B). Thus, *Prss16* is not required for normal surface expression of MHC class II on cTEC.

Analysis of T-lymphocyte populations. The effect of *Prss16* disruption on the development of T cells was evaluated by FACS analysis of T lymphocytes in the thymus and spleen of 4-to-6-week-old mice. Thymus weight and cellularity were not significantly different for *Prss16*$^{-/-}$ mice compared to wild-type and heterozygous mice. Both frequencies and total num-
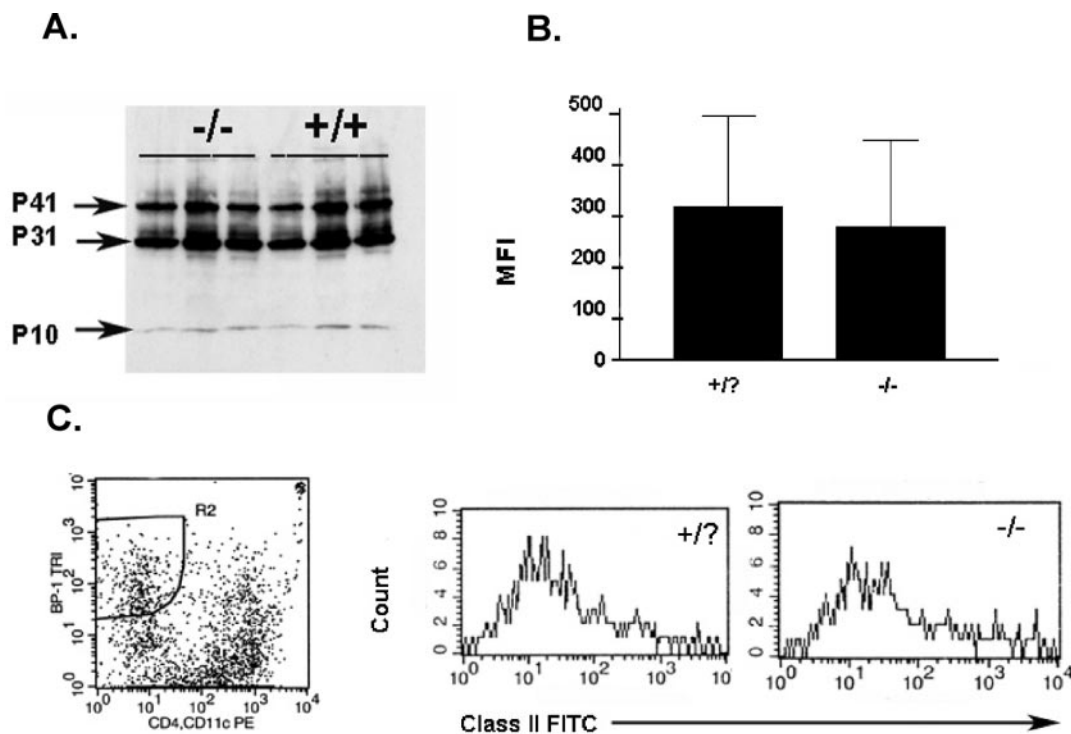
FIG. 2. (A) Western blot analysis with anti-Ii antibody (In-1) reveals no difference in Ii isoforms p41 and p31 and the degradation product p10 in thymic stromal cells of $Prss16^{-/-}$ mice compared to those of wild-type mice. The genotype of each animal is indicated. (B) MHC class II surface expression on BP-1$^+$CD4$^-$CD11c$^-$ cells. Shown are means and standard errors of the means. Wild-type and heterozygous animals were grouped together ($Prss16^{+/?}$), cTEC were identified by gating on low-density thymic cells that were BP-1$^+$CD4$^-$CD11c$^-$, and surface expression of MHC class II was estimated by mean fluorescence intensity (MFI). No significant difference was detected between $Prss16^{-/-}$ mice and their littermate controls ($n = 8$ per group). (C) Representative results of flow cytometry of low-density thymic cells stained for BP-1, CD4, CD11c, and MHC class II.

bers of CD4$^-$CD8$^-$, CD4$^+$CD8$^+$, CD4$^+$CD8$^-$, and CD4$^-$CD8$^+$ thymocytes were not significantly affected by the deletion of $Prss16$ (Fig. 3A). Similarly, the weight and cellularity of the spleen as well as the numbers and frequencies of CD4$^+$ and CD8$^+$ T cells were not different for the $Prss16^{-/-}$ mice (Fig. 3B).

To assess whether $Prss16$ is important in the early development of thymocytes prior to positive selection, we studied the CD3$^-$ population of thymocytes for expression of CD44 and CD25 (Fig. 3C). Prior to positive selection, thymocytes progress through a series of developmental steps characterized by CD44$^+$CD25$^-$, CD44$^+$CD25$^+$, and CD44^{low}CD25$^+$. The frequencies of these populations in $Prss16^{-/-}$ mice (0.86, 0.12, and 1.08%, respectively) were not significantly different than those in controls (0.91, 0.14, and 1.2%, respectively), indicating normal maturation and differentiation of thymocytes prior to positive selection.

Because of the potential link of $Prss16$ with type 1 diabetes and celiac disease, we studied populations of T cells implicated in autoimmunity. Specifically, we examined CD4$^+$CD25$^+$ T cells, NK T cells, and CD4$^-$CD8$^-$TCR$^+$ thymocytes, which have been implicated in the development of autoimmunity in NOD mice (14, 15, 33). Again, $Prss16^{-/-}$ mice had numbers of CD4$^+$CD25$^+$ T cells that were similar to those for control mice (Fig. 4A). In addition, no differences in CD4$^-$CD8$^-$TCR$^+$ thymocytes were detected (data not shown). Finally, NK T cells determined as DX5$^+$TCR$^+$ cells were found at similar frequencies in the spleens of $Prss16^{-/-}$ mice and controls (Fig. 4B).

Analysis of T-cell activation. Finally, we determined whether $Prss16^{-/-}$ T cells proliferate normally in response to TCR cross-linking. We did not find any significant difference in T-cell proliferation between $Prss16^{-/-}$ mice and controls when activated either by anti-CD3 or by concanavalin A (Fig. 5).

DISCUSSION

$PRSS16$ is a potentially important gene in the development of T cells and autoimmunity, but its function is unknown. Its specific expression in cortical epithelial cells of the thymus, predicted protease function, and encoding in the telomeric MHC class I region linked to autoimmune diseases all suggest a critical role in the positive selection of the TCR repertoire. We sought to begin to understand the in vivo function of $Prss16$ through the generation of $Prss16$-deficient mice. Mice carrying a null mutation of the $Prss16$ gene were generated by homologous recombination in ES cells, and, although we do not have a functional assay for Prss16 activity, residual Prss16 activity is unlikely for two reasons. First, the homologous recombination removed the putative active serine site in exon 5. Second, we confirmed that $Prss16$ RNA in the thymus was completely lacking in homozygous mutant mice.

Despite the absence of $Prss16$, mice are healthy and fertile in the expected Mendelian ratios. They also appear phenotypically normal and fail to exhibit any distinct anatomical or histological abnormality. Therefore, we conclude that $Prss16$ is not essential for embryonic or adult development or sexual
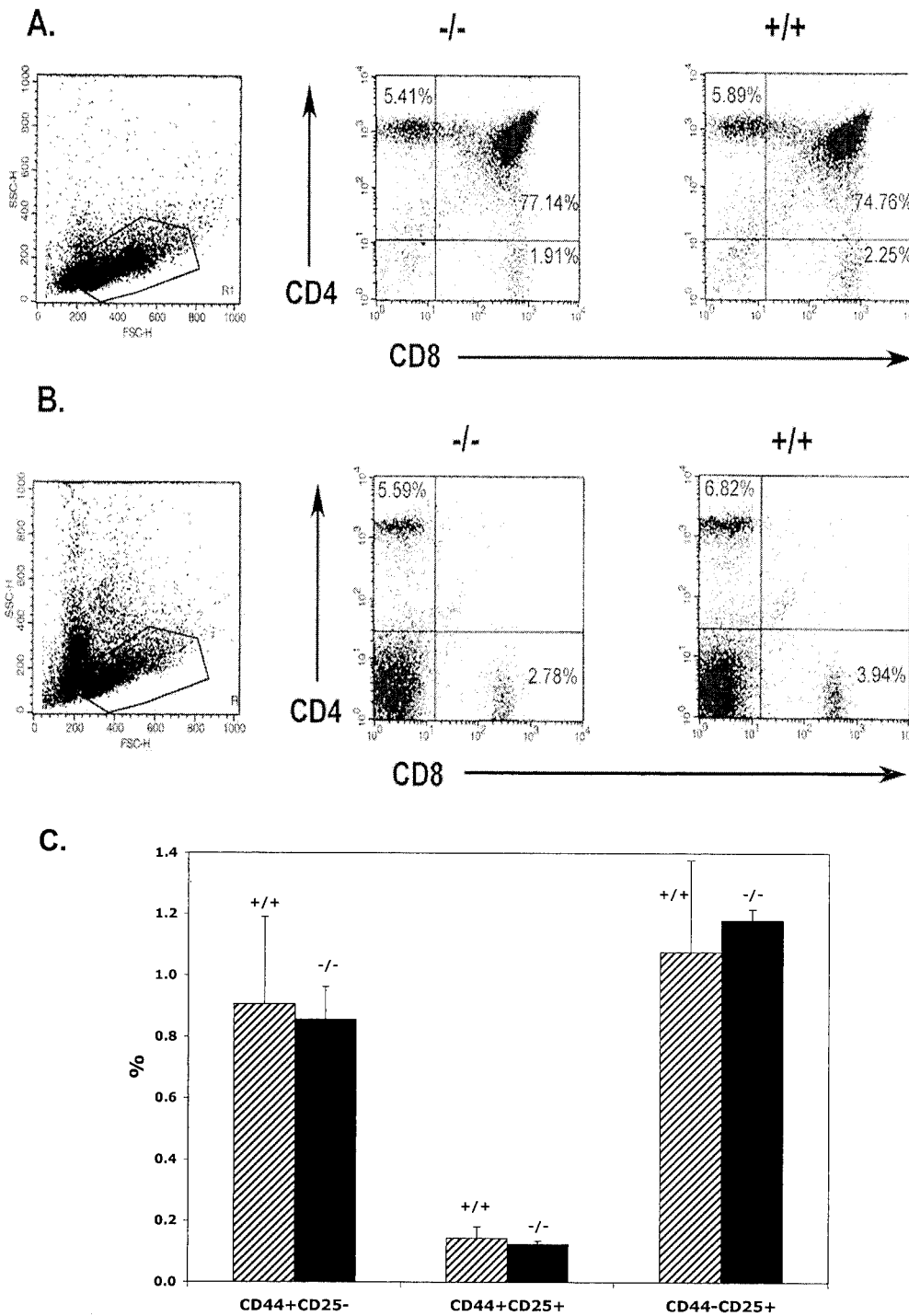
FIG. 3. The percentages and total numbers of CD4$^+$-, CD8$^+$-, and CD4$^+$CD8$^+$-T-cell populations are similar for *Prss16*$^{-/-}$ and *Prss16*$^{+/+}$ mice. Thymocytes (A) and splenocytes (B) from *Prss16*$^{-/-}$ and *Prss16*$^{+/+}$ littermates were stained with anti-CD4 and anti-CD8 monoclonal antibodies (MAb). The percentage of the total number of T cells in each population is indicated. The total numbers of T cells in the thymus and spleen of *Prss16*$^{-/-}$ mice did not differ significantly. (C) The percentage of CD3$^-$ thymocytes expressing CD44, CD25, or both did not differ significantly between *Prss16*$^{-/-}$ (solid bar) and *Prss16*$^{+/+}$ (hatched bar) littermates. Thymocytes were stained with anti-CD3, anti-CD44, and anti-CD25 MAb. The CD3$^-$ population was gated for analysis of CD44 and CD25. The percentage of the total number of T cells in each population is indicated.

maturation of mice, nor is it required for normal anatomical development of the thymus.

cTEC in the thymus play a central role in positive selection by processing and presenting self-antigens bound to MHC class II, which interact with the TCR of thymocytes and facilitate the selection of MHC-restricted TCR (2, 19). Recently, diversity in MHC class II antigen processing pathways has been recognized. Differences dependent upon the antigen and the
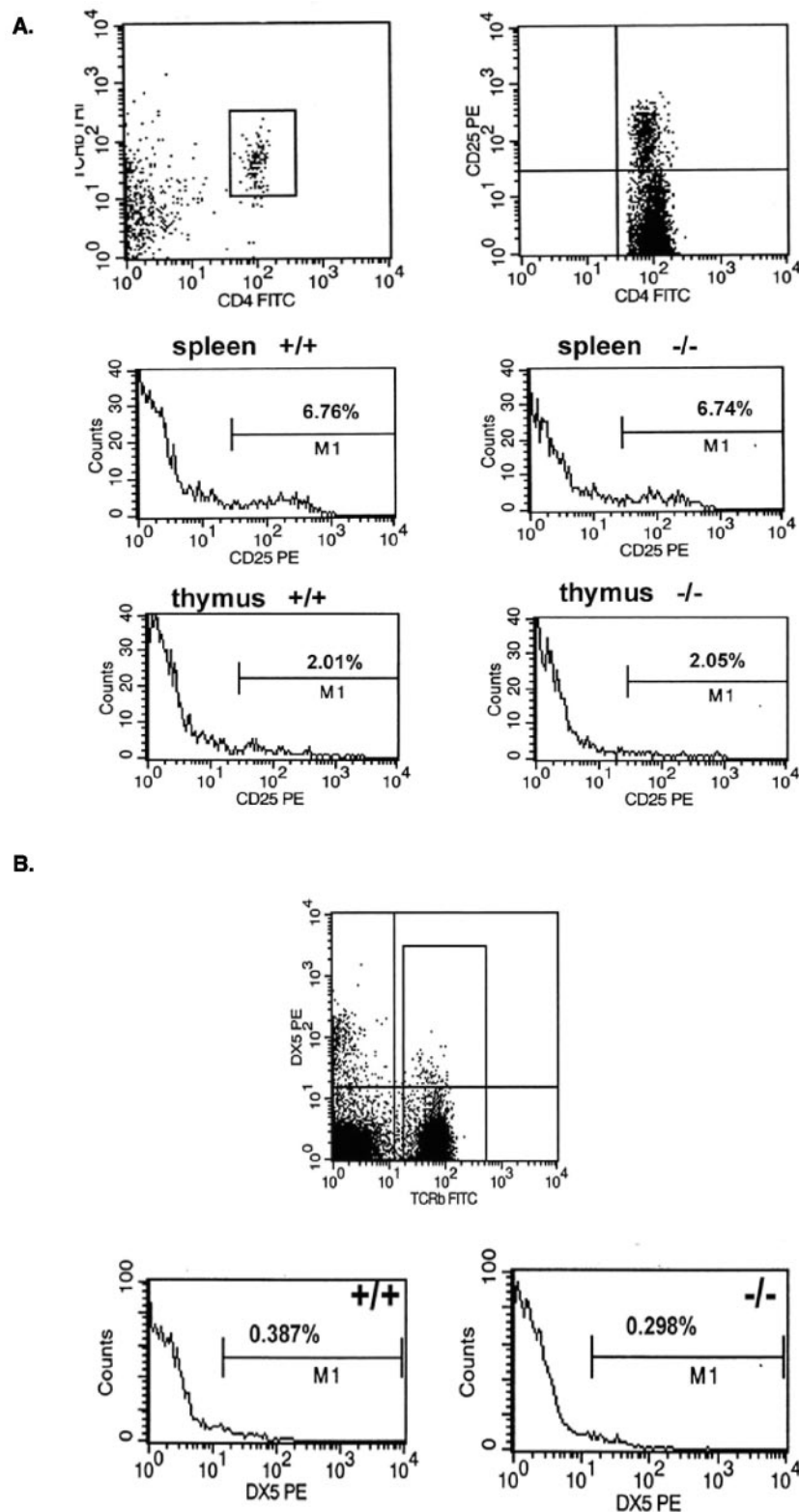
FIG. 4. (A) The percentages of thymic and splenic CD4$^+$CD25$^+$ T cells were not affected by deletion of *Prss16*. Splenic and thymic cells of *Prss16*$^{+/+}$ and *Prss16*$^{-/-}$ mice were stained with anti-TCRβ, anti-CD4, and anti-CD25. The percentages of TCRβ$^+$CD4$^+$ cells expressing CD25 are indicated. (B) NK T cells identified as TCRβ$^+$DX5$^+$ from spleens of *Prss16*$^{+/+}$ and *Prss16*$^{-/-}$ mice were analyzed by using three-color FACS analysis. The numbers indicate the percentages of DX5$^+$ T cells.
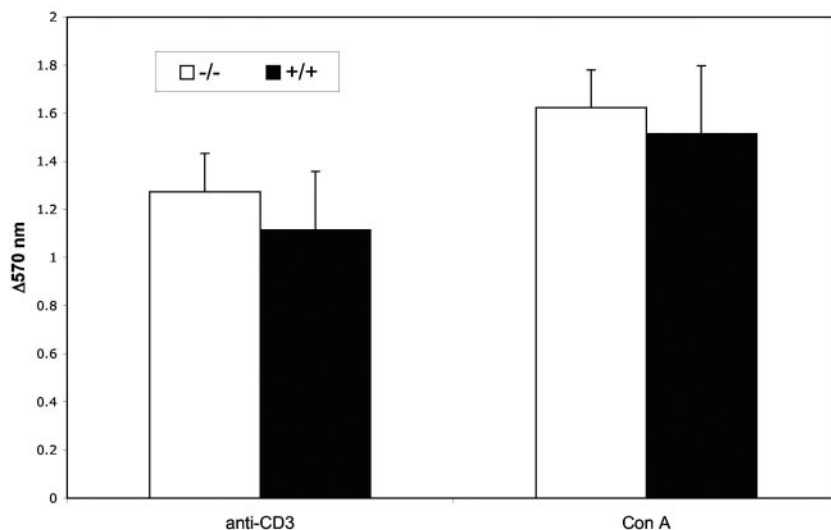
FIG. 5. Activation of splenocytes by anti-CD3 MAb and concanavalin A from *Prss16*^{−/−} mice is not different from that from control littermates. Splenocytes were treated for 48 h with either anti-CD3 MAb or concanavalin A, and proliferation was assessed by an MTT assay. Bars represent the means ± standard deviations of the differences in absorbance at 570 nm between anti-CD3-, concanavalin A-, and PBS-treated cells. Each group of 10 mice was assayed in triplicate.

antigen-presenting cell type have been identified in both the proteolytic milieu and the cellular compartments involved. In typical APC, MHC class II αβ heterodimers are synthesized and assembled in the endoplasmic reticulum with the assistance of invariant chain. A trimer of Ii binds three αβ heterodimers and protects the empty groove of MHC class II from premature binding of peptide antigen and directs the MHC-Ii complexes to endosomal/lysosomal compartments. Ii then undergoes proteolytic degradation primarily by cathepsin S, ultimately resulting in the class II-associated invariant chain peptide fragment, which remains bound in the MHC class II antigen binding groove until being replaced by antigen with the aid of HLA-DM.

cTEC lines are very poor processors of exogenous antigen, perhaps related to the fact that the MHC class II loading compartment appears to be in early endosomes as opposed to the endosomes/lysosomes. Differences also exist in the proteases responsible for the degradation of Ii chain, which is due at least in part to the activity of cathepsin L in mice and of cathepsin V in humans (23, 30). These proteases are specific to cTEC and are not found in medullary TEC or dendritic cells. Furthermore, loss of cathepsin L function results in impaired Ii degradation and positive selection of CD4^{+} T cells and NK T cells (17, 23).

To study the effect of *Prss16* on the MHC class II presentation pathway, we measured the surface expression of MHC class II on cTEC. We found that *Prss16* deficiency did not affect the level of MHC class II on cTEC. However, cathepsin L-deficient mice also express normal amounts of MHC class II but have incomplete degradation of Ii. Therefore, we also analyzed the degradation products of Ii protein in *Prss16*^{−/−} mice and their littermate controls but found that disruption of *Prss16* did not affect Ii degradation.

T-cell subpopulations were also determined to be nearly identical for the wild-type and mutant mice. In the thymus, these subpopulations included double-positive CD4^{+}CD8^{+} and single-positive CD4^{+} and CD8^{+} cells as well as more immature thymocytes. Additionally, similar proportions of mature CD4^{+} and CD8^{+} T cells were present in the spleens of control and *Prss16*^{−/−} mice. Furthermore, the CD4^{+}CD25^{+}- and DX5^{+}-T-cell populations, which play an important role in the regulation of autoimmune diseases (26), were not significantly different between *Prss16*^{−/−} and control animals. Finally, T cells respond normally to activation in *Prss16*^{−/−} mice. Thus, loss of *Prss16* function does not quantitatively alter T-cell populations or the ability of T cells to proliferate.

The lack of a significant effect of *Prss16* deficiency on MHC expression and T-cell numbers is not completely surprising. The predicted protein of *Prss16* has similarity with prolylcarboxypeptidase, which cleaves the carboxy-terminal amino acid of proteins with a proline in the penultimate position. This predicted function, along with our present findings, suggests that *Prss16* is not involved in the endoproteolytic cleavage of Ii. Rather, it may be involved in the editing of COOH-terminal residues of peptide antigens. These COOH-terminal peptide flanking residues have previously been shown to enhance MHC binding (27). In addition, many CD4^{+} T cells generated by hen egg lysozyme epitopes are dependent upon these residues (3). Moreover, dependence on these residues correlates with usage of TCR V beta (8). Thus, the effect of *Prss16* deficiency may be subtle and only alter a specific subset of peptide antigens and the resulting T-cell repertoire.

One of the primary reasons for interest in *Prss16* is based upon its linkage to autoimmune diseases. Lie et al. analyzed transmission of alleles from parents homozygous for the susceptible *HLA-DR3* haplotype to children with type 1 diabetes and found that the frequency of transmission of allele 3 at *D6S2223* was significantly reduced (21). In addition, the frequency of *D6S2223* allele 3 in individuals homozygous for *HLA-DR3* is significantly greater in healthy controls than in individuals with type I diabetes or celiac disease (20). Interestingly, PRSS16 is the only gene product encoded in this region with a clearly immunologic function. However, no mutations in *Prss16* have yet been clearly linked to type 1 diabetes.

In conclusion, *Prss16* is not required for the expression of MHC class II on cTEC or for the development of normal numbers of T cells. Future studies are required to determine whether *Prss16* plays a more prominent role in the presence of autoimmune-prone MHC alleles. In addition, the function of *Prss16* in shaping the peptide repertoire and thus the positive selection of T cells also deserves further study.

ACKNOWLEDGMENTS

REFERENCES

1. **Anderson, G., and E. J. Jenkinson.** 2001. Lymphostromal interactions in thymic development and function. Nat. Rev. Immunol. **1:**31–40.
2. **Anderson, G., J. J. Owen, N. C. Moore, and E. J. Jenkinson.** 1994. Thymic epithelial cells provide unique signals for positive selection of CD4+CD8+ thymocytes in vitro. J. Exp. Med. **179:**2027–2031.
3. **Arnold, P. Y., N. L. La Gruta, T. Miller, K. M. Vignali, P. S. Adams, D. L. Woodland, and D. A. Vignali.** 2002. The majority of immunogenic epitopes generate CD4+ T cells that are dependent on MHC class II-bound peptide-flanking residues. J. Immunol. **169:**739–749.
4. **Baldwin, K. K., B. P. Trenchak, J. D. Altman, and M. M. Davis.** 1999. Negative selection of T cells occurs throughout thymic development. J. Immunol. **163:**689–698.
5. **Barton, G. M., and A. Y. Rudensky.** 1999. Requirement for diverse, low-abundance peptides in positive selection of T cells. Science **283:**67–70.
6. **Berg, L. J., B. Fazekas de St. Groth, A. M. Pullen, and M. M. Davis.** 1989. Phenotypic differences between αβ versus β T-cell receptor transgenic mice undergoing negative selection. Nature **340:**559–562.
7. **Bowlus, C. L., J. Ahn, T. Chu, and J. R. Gruen.** 1999. Cloning of a novel MHC-encoded serine peptidase highly expressed by cortical epithelial cells of the thymus. Cell. Immunol. **196:**80–86.
8. **Carson, R. T., K. M. Vignali, D. L. Woodland, and D. A. Vignali.** 1997. T cell receptor recognition of MHC class II-bound peptide flanking residues enhances immunogenicity and results in altered TCR V region usage. Immunity **7:**387–399.
9. **Cheunsuk, S., R. Sparks, J. K. Noveroske, T. Hsu, M. J. Justice, M. E. Gershwin, J. R. Gruen, and C. L. Bowlus.** 2002. Expression, genomic structure and mapping of the thymus specific protease *Prss16*: a candidate gene for insulin dependent diabetes mellitus susceptibility. J. Autoimmun. **18:**311–316.
10. **Farr, A. G., D. J. Eisenhardt, and S. K. Anderson.** 1986. Isolation of murine thymic epithelium and an improved method for its propagation in vitro. Anat. Rec. **216:**85–94.
11. **Fink, P. J., and M. J. Bevan.** 1978. H-2 antigens of the thymus determine lymphocyte specificity. J. Exp. Med. **148:**766–775.
12. **Fukui, Y., T. Ishimoto, M. Utsuyama, T. Gyotoku, T. Koga, K. Nakao, K. Hirokawa, M. Katsuki, and T. Sasazuki.** 1997. Positive and negative CD4+ thymocyte selection by a single MHC class II/peptide ligand affected by its expression level in the thymus. Immunity **6:**401–410.
13. **Gapin, L., Y. Fukui, J. Kanellopoulos, T. Sano, A. Casrouge, V. Malier, E. Beaudoing, D. Gautheret, J. M. Claverie, T. Sasazuki, and P. Kourilsky.** 1998. Quantitative analysis of the T cell repertoire selected by a single peptide-major histocompatibility complex. J. Exp. Med. **187:**1871–1883.
14. **Godfrey, D. I., S. J. Kinder, P. Silvera, and A. G. Baxter.** 1997. Flow cytometric study of T cell development in NOD mice reveals a deficiency in αβTCR+CDR−CD8− thymocytes. J. Autoimmun. **10:**279–285.
15. **Hammond, K. J., D. G. Pellicci, L. D. Poulton, O. V. Naidenko, A. A. Scalzo, A. G. Baxter, and D. I. Godfrey.** 2001. CD1d-restricted NKT cells: an inter-strain comparison. J. Immunol. **167:**1164–1173.
16. **Hogquist, K. A., A. J. Tomlinson, W. C. Kieper, M. A. McGargill, M. C. Hart, S. Naylor, and S. C. Jameson.** 1997. Identification of a naturally occurring ligand for thymic positive selection. Immunity **6:**389–399.
17. **Honey, K., K. Benlagha, C. Beers, K. Forbush, L. Teyton, M. J. Kleijmeer, A. Y. Rudensky, and A. Bendelac.** 2002. Thymocyte expression of cathepsin L is essential for NKT cell development. Nat. Immunol. **3:**1069–1074.
18. **Kasai, M., E. Kominami, and T. Mizuochi.** 1998. The antigen presentation pathway in medullary thymic epithelial cells, but not that in cortical thymic epithelial cells, conforms to the endocytic pathway. Eur. J. Immunol. **28:**1867–1876.
19. **Kisielow, P., H. S. Teh, H. Bluthmann, and H. von Boehmer.** 1988. Positive selection of antigen-specific T cells in thymus by restricting MHC molecules. Nature **335:**730–733.
20. **Lie, B. A., L. M. Sollid, H. Ascher, J. Ek, H. E. Akselsen, K. S. Rønningen, E. Thorsby, and D. E. Undlien.** 1999. A gene telomeric of the HLA class I region is involved in predisposition to both type 1 diabetes and coeliac disease. Tissue Antigens **54:**162–168.
21. **Lie, B. A., J. A. Todd, F. Pociot, J. Nerup, H. E. Akselsen, G. Joner, K. Dahl-Jørgensen, K. S. Rønningen, E. Thorsby, and D. E. Undlien.** 1999. The predisposition to type 1 diabetes linked to the human leukocyte antigen complex includes at least one non-class II gene. Am. J. Hum. Genet. **64:**793–800.
22. **Mizuochi, T., M. Kasai, T. Kokuho, T. Kakiuchi, and K. Hirokawa.** 1992. Medullary but not cortical thymic epithelial cells present soluble antigens to helper T cells. J. Exp. Med. **175:**1601–1605.
23. **Nakagawa, T., W. Roth, P. Wong, A. Nelson, A. Farr, J. Deussing, J. A. Villadangos, H. Ploegh, C. Peters, and A. Y. Rudensky.** 1998. Cathepsin L: critical role in Ii degradation and CD4 T cell selection in the thymus. Science **280:**450–453.
24. **Oukka, M., P. Andre, P. Turmel, N. Besnard, V. Angevin, L. Karlsson, P. L. Trans, D. Charron, B. Bihain, K. Kosmatopoulos, and V. Lotteau.** 1997. Selectivity of the major histocompatibility complex class II presentation pathway of cortical thymic epithelial cell lines. Eur. J. Immunol. **27:**855–859.
25. **Robinson, J. H., and A. A. Delvig.** 2002. Diversity in MHC class II antigen presentation. Immunology **105:**252–262.
26. **Sakaguchi, S.** 2000. Regulatory T cells: key controllers of immunologic self-tolerance. Cell **101:**455–458.
27. **Sant'Angelo, D. B., E. Robinson, C. A. Janeway, Jr., and L. K. Denzin.** 2002. Recognition of core and flanking amino acids of MHC class II-bound peptides by the T cell receptor. Eur. J. Immunol. **32:**2510–2520.
28. **Sant'Angelo, D. B., P. G. Waterbury, B. E. Cohen, W. D. Martin, L. Van Kaer, A. C. Hayday, and C. A. Janeway, Jr.** 1997. The imprint of intrathymic self-peptides on the mature T cell receptor repertoire. Immunity **7:**517–524.
29. **Shi, G. P., R. A. Bryant, R. Riese, S. Verhelst, C. Driessen, Z. Li, D. Bromme, H. L. Ploegh, and H. A. Chapman.** 2000. Role for cathepsin F in invariant chain processing and major histocompatibility complex class II peptide loading by macrophages. J. Exp. Med. **191:**1177–1186.
30. **Tolosa, E., W. Li, Y. Yasuda, W. Wienhold, L. K. Denzin, A. Lautwein, C. Driessen, P. Schnorrer, E. Weber, S. Stevanovic, R. Kurek, A. Melms, and D. Bromme.** 2003. Cathepsin V is involved in the degradation of invariant chain in human thymus and is overexpressed in myasthenia gravis. J. Clin. Investig. **112:**517–526.
31. **Tourne, S., T. Miyazaki, A. Oxenius, L. Klein, T. Fehr, B. Kyewski, C. Benoist, and D. Mathis.** 1997. Selection of a broad repertoire of CD4+ T cells in H-2Ma0/0 mice. Immunity **7:**187–195.
32. **Villadangos, J. A., R. A. Bryant, J. Deussing, C. Driessen, A. M. Lennon-Dumenil, R. J. Riese, W. Roth, P. Saftig, G. P. Shi, H. A. Chapman, C. Peters, and H. L. Ploegh.** 1999. Proteases involved in MHC class II antigen presentation. Immunol. Rev. **172:**109–120.
33. **Wu, A. J., H. Hua, S. H. Munson, and H. O. McDevitt.** 2002. Tumor necrosis factor-α regulation of CD+CD25+ T cell levels in NOD mice. Proc. Natl. Acad. Sci. USA **99:**12287–12292.